Effect of Nonlinear Electron Landau Damping in Collisionless Drift-Wave Turbulence

Frank Jenko and Bruce D. Scott
Max-Planck-Institut für Plasmaphysik, EURATOM Association, Boltzmannstraße 2, 85748 Garching, Germany
(Received 29 July 1997; revised manuscript received 24 December 1997)

Collisionless drift-wave turbulence is studied with numerical simulations in a three-dimensional sheared slab geometry. Nonlinear electron Landau damping associated with parallel trapping is found to substantially reduce the anomalous particle transport for low magnetic shear ($\hat{s} < 1$), whereas it plays a very weak role for higher shear ($\hat{s} > 1$). This result has implications for the construction of transcollisional Landau-fluid models for passing electrons in the edge ($r/a > 0.8$) of a tokamak. [S0031-9007(98)06253-X]

PACS numbers: 52.35.Ra, 52.35.Kt, 52.65.–y

There is experimental evidence that the anomalous transport in tokamak plasmas can be attributed to drift-wave turbulence in certain parameter regimes [1]. In the steep gradient zone of a tokamak edge ($r/a > 0.8$) the passing electrons are at most weakly collisional so that parallel electron Landau damping plays a crucial role in the drift-wave dynamics. To avoid a fully kinetic treatment, transcollisional Landau-fluid models [2,3] have been proposed to retain this important kinetic effect. While *linear* Landau damping in the parallel electron dynamics can already be captured by these Landau-fluid models [2–5], the corresponding nonlinear effect (i.e., electrostatic trapping associated with the velocity-space nonlinearity in the electron drift-kinetic equation) may be much harder to incorporate. Earlier work by Lee *et al.* [6] in a two-dimensional shearless slab geometry has shown that nonlinear electron Landau damping can play an important role in determining the level of the fluctuations in collisionless drift-wave turbulence. In the following, we present well-resolved computations studying this effect in a more realistic three-dimensional sheared slab geometry.

In a strongly magnetized, collisionless plasma (i.e., $\nu_e \ll \omega \ll \Omega_i$ where ν_e and Ω_i are, respectively, the electron collision frequency and the ion cyclotron frequency) the electron dynamics can be described by the drift-kinetic Vlasov equation [7] which reads in slab geometry

$$\frac{\partial f_e}{\partial t} + \mathbf{v}_E \cdot \nabla_\perp f_e + w_\parallel \nabla_\parallel f_e - \frac{e}{m_e} E_\parallel \frac{\partial f_e}{\partial w_\parallel} = 0 \,. \quad (1)$$

Here $f_e(\mathbf{r}, w_\parallel, t)$ denotes the distribution function for the electron guiding centers, $\mathbf{v}_E = (c/B^2)\mathbf{E} \times \mathbf{B}$ is the $\mathbf{E} \times \mathbf{B}$ drift velocity, $-e$ and m_e are, respectively, the electron charge and mass, and w is the velocity. $\parallel$ and $\perp$ denote the directions parallel and perpendicular to the magnetic field $\mathbf{B}$. Note that in a slab model, $w_\perp$ space can be integrated out, so that the computational velocity space is one dimensional. In the electrostatic limit the electric field is given by $\mathbf{E} = -\nabla\phi$, where ϕ is the electrostatic potential.

We treat the ions as a cold fluid, such that their drift velocity is $\mathbf{v}_E$ and their parallel velocity, $u_\parallel$, results from $E_\parallel$. Quasineutrality is maintained by the ion polarization current, so that $\nabla \cdot \mathbf{J} = 0$ for the total current $\mathbf{J}$, with $J_\parallel = enu_\parallel - e \int w_\parallel f_e \, d^3w$ and $\mathbf{J}_\perp = en(c/\Omega_i B) d\mathbf{E}_\perp/dt$, where n is the plasma density. This constraint determines the time dependence of ϕ and hence $\mathbf{v}_E$. Unfortunately, the term "nonlinear Landau damping" is somewhat ambigious; it is used to describe both parallel electron trapping and perpendicular ion trapping (associated with $\mathbf{v}_E \cdot \nabla_\perp f_i$) which can also be important in collisionless drift-wave turbulence [6]. In our model, $\mathbf{E} \times \mathbf{B}$ advection is retained in the equations for n and $u_\parallel$ which are all the ion moments present. As we are investigating electron dynamics, this simplification is justified for the development of a transcollisional fluid description of passing electrons.

Under drift ordering, f_e is split into a background Maxwellian, f_m, and a fluctuating part, $\tilde{f}$. The density profile gradient (here we neglect ∇T_e) appears in f_m but is retained only in $\mathbf{v}_E \cdot \nabla f_m$. Defining the electron thermal velocity $v_T = \sqrt{2T_e/m_e}$, the ion sound speed $c_s = \sqrt{T_e/M_i}$, and the drift-wave dispersion scale $\rho_s = \sqrt{M_i T_e}\, c/eB$, the dependent variables are normalized according to $(\tilde{f} v_T^3/n)\delta^{-1} \mapsto f$, $(e\phi/T_e)\delta^{-1} \mapsto \phi$, and $(u_\parallel/c_s)(L_n/qR)\delta^{-1} \mapsto u_\parallel$, where $\delta = \rho_s/L_n$. Here, T_e is the electron temperature, M_i is the ion mass, L_n is the density profile scale length, and $2\pi qR$ is the magnetic field line connection length. The independent variables are scaled as $x/\rho_s \mapsto x$, $y/\rho_s \mapsto y$, $z/qR \mapsto z$, $w/v_T \mapsto w$, and $tc_s/L_n \mapsto t$. The dimensionless equations for f, ϕ, and $u_\parallel$ are then given by

$$\frac{df}{dt} = -f_m \frac{\partial \phi}{\partial y} - \alpha_e w_\parallel \nabla_\parallel (f - f_m \phi) - \frac{\delta}{2} \alpha_e \frac{\partial f}{\partial w_\parallel} \nabla_\parallel \phi \,, \quad (2)$$

$$\frac{d}{dt} \nabla_\perp^2 \phi = \nabla_\parallel \left(u_\parallel - \int \alpha_e w_\parallel f \, d^3w \right), \quad (3)$$

$$\hat{\epsilon}_s \frac{du_\parallel}{dt} = -\nabla_\parallel \phi + \mu_\parallel \nabla_\parallel^2 u_\parallel \,, \quad (4)$$

where

$$\frac{d}{dt} = \frac{\partial}{\partial t} + \mathbf{v}_E \cdot \nabla_\perp = \frac{\partial}{\partial t} - \frac{\partial \phi}{\partial y}\frac{\partial}{\partial x} + \frac{\partial \phi}{\partial x}\frac{\partial}{\partial y}, \quad (5)$$

and $f_m = \pi^{-3/2} e^{-w^2}$. In Eq. (4) we have added a parallel viscosity, $\mu_\parallel$ which serves as a crude model for ion Landau damping. The most important parameter in the present electrostatic collisionless model is $\alpha_e = (L_n/qR)(2M_i/m_e)^{1/2}$, which is given by the ratio of the parallel to the perpendicular dynamical frequencies, i.e., thermal electron transit frequency v_T/qR to drift frequency c_s/L_n. The parameter $\hat{\epsilon}_s = (qR/L_n)^2$, which controls the ion inertia, is secondary.

The coordinate system (x, y, z) is aligned to the background gradient and magnetic field, which is modeled as a sheared slab by taking $\mathbf{B} = B[\nabla z - (x/L_s)\nabla y]$, where $L_s = qR/\hat{s}$ is the shear length. The orientation is $\nabla x \propto -\nabla n$ and $\nabla x \times \nabla y \cdot \nabla z = 1$. Alignment to $\mathbf{B}$ is done by transforming y such that $\mathbf{B} \cdot \nabla y = 0$, which gives $x \mapsto x$, $y + xz/L_s \mapsto y$, and $z \mapsto z$, leaving $\nabla_\parallel = \partial/\partial z$. The nonorthogonal property of this coordinate system is reflected in the metric [8]

$$\nabla_\perp^2 = \left(\frac{\partial}{\partial x} + \hat{s}z\frac{\partial}{\partial y}\right)^2 + \left(\frac{\partial}{\partial y}\right)^2 \quad (6)$$

and in the parallel boundary condition [9–11]

$$S(x, y, z + 2\pi) = S(x, y - 2\pi\hat{s}x, z) \quad (7)$$

for any scalar quantity S. In the perpendicular (x, y) plane, periodic boundary conditions are applied.

Numerically, we use a nonlinear Vlasov code which is based on a finite-difference scheme for the electron distribution function. The velocity-space nonlinearity in the drift-kinetic equation becomes more important with increasing δ. We usually set $\delta = 0.02$ which is a large but realistic value. The other simulation parameters were the following. The computational domain was $32\rho_s \times 64\rho_s \times 2\pi qR$; the total simulation time was up to $2000 L_n/c_s$. This corresponds to about 3 cm $\times$ 6 cm and 2 ms for typical tokamak conditions. $w_\parallel$ ran from $-3v_T$ to $3v_T$. The grid was typically $32 \times 64 \times 16 \times 100$ nodes in $(x, y, z, w_\parallel)$ space. The initial condition for the distribution function f was a localized disturbance in real space and a Maxwellian in velocity space, whereas ϕ and $u_\parallel$ were both set to zero.

To get a better understanding of the turbulent system, one can construct energylike expressions in terms of squared fluctuating quantities, e.g.,

$$E_n = \frac{1}{2}\langle n^2 \rangle, \qquad E_\phi = \frac{1}{2}\langle v_E^2 \rangle, \quad (8)$$

where $n = \int f\, d^3w$ is the zeroth moment of the electron distribution function, and $\langle \cdots \rangle = V^{-1}\int \cdots d^3r$ denotes spatial averaging. Other terms could be defined similarly [12] but for the following discussion, E_n and E_ϕ are sufficient. Using the above equations (2) and (3), one can calculate their time derivatives,

$$\dot{E}_n = \Gamma_n - \langle n \nabla_\parallel v_\parallel \rangle, \qquad \dot{E}_\phi = \langle \phi \nabla_\parallel (v_\parallel - u_\parallel) \rangle, \quad (9)$$

where $v_\parallel = \int \alpha_e w_\parallel f\, d^3w$ is the first moment of the electron distribution function. The term $\Gamma_n = -\langle n\, \partial\phi/\partial y \rangle$ acts as a source for E_n and drives the turbulence by extracting energy from the background density gradient and putting it into the density fluctuations. At the same time it measures the particle transport in the radial direction. In terms of spectra, $\Gamma_n(N)$ will refer to the contribution of a given parallel wave number $k_\parallel$ to Γ_n [13]. Noting that $n \approx \phi$ for drift waves, it is clear that energy is transferred from E_n to E_ϕ through parallel compression.

Let us first examine the case with an unsheared magnetic field (see Fig. 1). If one starts out with a density fluctuation amplitude well below unity, the system first goes through a linear phase in which the nonlinear terms are negligible and the various modes in the system are not coupled to each other. As expected, it turns out that the system is quickly dominated by the most unstable mode, $N = 1$ in our case, where the mode numbers N are given by $N = k_\parallel qR$. Free energy E_n is tapped via the linear instability (1) and put into E_ϕ through drift-wave equipartition (2). In the subsequent nonlinear phase, fluctuation energy E_ϕ is transferred from the $N = 1$ modes (drift waves) to $N = 0$ modes (convective cells, not drift waves) through the inverse energy cascade (3). This mechanism is caused by the $\mathbf{E} \times \mathbf{B}$ nonlinearity in the vorticity equation, as was inferred from another run where it was turned off. And although there is no direct coupling between the density and the potential fluctuations for $N = 0$, energy can now be extracted from the background gradient and put into E_n through passive

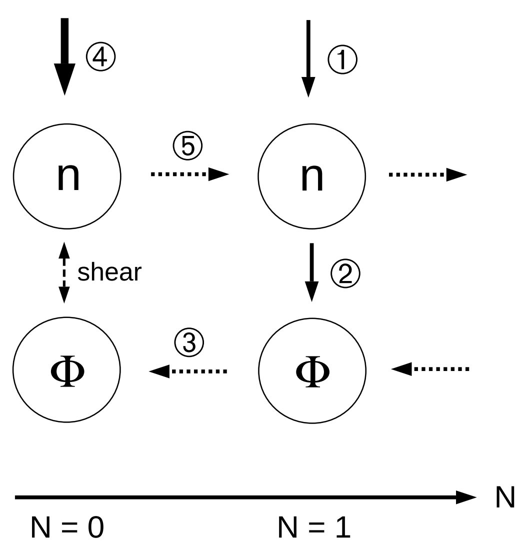

FIG. 1. Energy transfer processes in parallel wave-number space $N = k_\parallel qR = 1, 2, \ldots$ for the case of an unsheared magnetic field. In the sheared system, $N = 0$ modes are also directly coupled to each other. The processes 1–5 are described in the text.

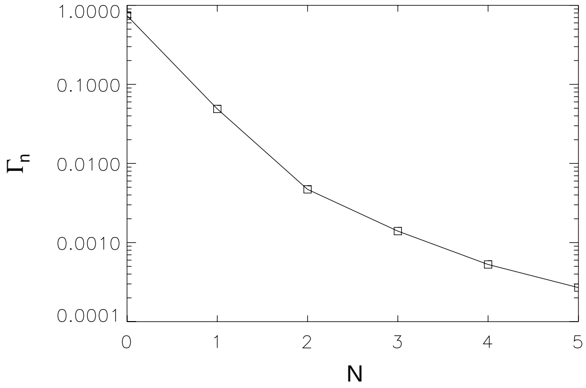

FIG. 2. Drive rate spectrum $\Gamma_n(N)$, $\Gamma_n = \sum_N \Gamma_n(N)$, in parallel wave-number space $N = k_\| qR = 0, 1, \ldots$ for the case of an unsheared magnetic field. More than 90% of the transport is caused by convective cells, i.e., modes with $N = 0$.

advection of the density (4). The $\mathbf{E} \times \mathbf{B}$ nonlinearity in the drift-kinetic equation then transfers density fluctuation energy back to the drift waves (5). This inherently nonlinear drive mechanism is mediated through energy transfer in $k_\|$ space and characterizes the physics of the turbulent system. It can be described as a coupling between drift waves and convective cells and has been seen before both in collisionless [14] and collisional [13] three-dimensional systems. During fully developed turbulence, more than 90% of the transport is indeed caused by convective cells, not drift waves, as can be seen in Fig. 2.

The velocity-space nonlinearity which is associated with the effect of nonlinear Landau damping has an impact on the parallel dynamics of the electrons and therefore on the properties of the drift wave system (see Fig. 3). Electrons whose kinetic energy is less than the electrostatic energy of the wave get trapped in the potential fluctuations and are forced to move along

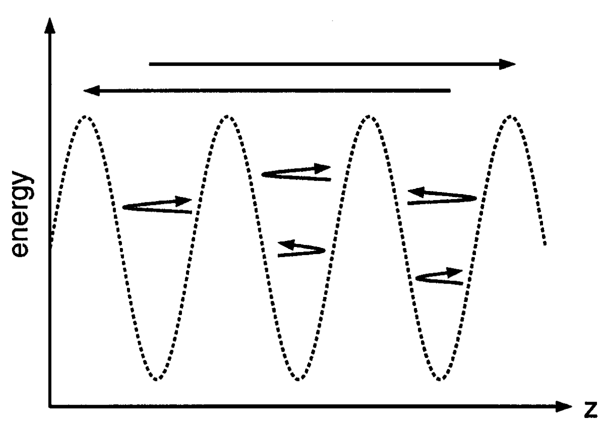

FIG. 3. Through the influence of the velocity-space nonlinearity, low-energetic electrons can get trapped in the drift-wave potential and are then forced to move along with the wave in the parallel direction.

with the wave in the parallel direction. Therefore the transport properties of the unsheared system are changed only indirectly as the velocity-space nonlinearity has no direct influence on the convective cells which control the transport level observed in the simulations to a large degree.

The effect of nonlinear electron Landau damping was studied quantitatively with numerical simulations. Each run was repeated (using the exact same set of physical parameters) with the velocity-space nonlinearity switched on. An example of the resulting time-averaged transport levels calculated from the simulations of the unsheared system is listed in Table I under run number 1. One observes a substantial suppression of anomalous transport which is accompanied by a decrease in the fluctuation level $\langle \phi^2 \rangle^{1/2}$ from 4.2 to 3.6. As the energy in E_ϕ enters only through E_n at finite $k_\|$, this shows that this linear energy transfer process is reduced by the velocity-space nonlinearity. Hence, less energy reaches the potential fluctuations with $N = 0$ and the drive via convective cells is weakened. Obviously, the self-consistent dynamical equilibria of the turbulent systems with and without nonlinear electron Landau damping are quite different from each other. It should again be stressed here that the homogeneous system consists of two subsystems, namely, the drift waves and the convective cells, which are only coupled through the $\mathbf{E} \times \mathbf{B}$ nonlinearities in the equations for f and ϕ. The subtle balance between the two clearly leads to a quite high sensitivity with respect to changes in the parallel part of the drift-wave dynamics.

In the case of a sheared magnetic field the basic equations are modified in two ways, as explained above. First, as potential fluctuations spread along the magnetic field lines, they are twisted due to the z dependence of the metric, as described by Eq. (6). Second, strict periodicity in z is broken by the field line connection, as described by Eq. (7). This means that for finite k_y the existence of strict $k_\| = 0$ modes is not allowed [11]. Rather, each mode has a finite parallel component which keeps n and ϕ directly coupled to each other, i.e., there are no longer any pure convective cells, just the drift waves. A $k_\|$ spectrum can still be described, but now N refers to the part of the spectrum with $k_\| qR$ between $N - 1/2$ and $N + 1/2$ [11]. Consequently, one can expect major differences to

TABLE I. Influence of nonlinear electron Landau damping on the particle transport Γ_n for $\delta = 0.02$. Γ_n' corresponds to the runs with the velocity-space nonlinearity switched on.

Run	$\hat{\mu} = 2/\alpha_e^2$	$\hat{s}$	Γ_n	Γ_n'	$(\Gamma_n' - \Gamma_n)/\Gamma_n$
1	0.3	0.0	0.80	0.50	−38%
2	10	0.32	0.52	0.36	−31%
3	10	0.64	0.21	0.16	−24%
4	10	0.95	0.098	0.081	−17%
5	10	1.27	0.041	0.037	−10%

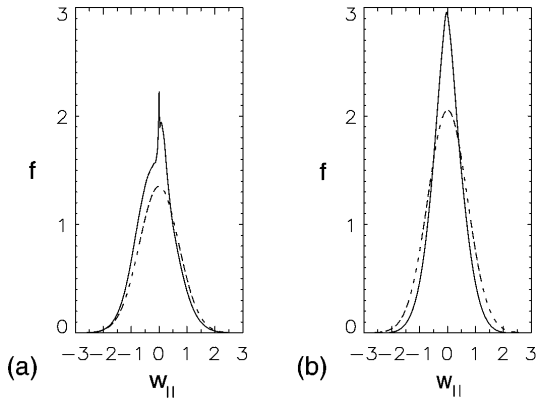

FIG. 4. Typical snapshots of $f(w_{\|})$ at a fixed point in space for runs (a) without and (b) with nonlinear electron Landau damping. The dashed lines show $f_m\phi$ for comparison.

the unsheared case as the $k_{\|}$ space scenario described above is no longer valid (see Fig. 1).

The simulations were started with a density fluctuation amplitude well above unity, and the system then relaxed towards a turbulent steady state which was driven nonlinearly [15–17] just as in the unsheared case. Again, all the runs were repeated with the velocity-space nonlinearity switched on. A signature of the impact that it has on the parallel electron dynamics can be seen in Fig. 4 which shows two typical snapshots of $f(w_{\|})$ at a fixed point in space for runs with and without nonlinear electron Landau damping. As parallel trapping is associated with diffusion in $w_{\|}$ space [18], one expects a smoothing of $f(w_{\|})$ which is indeed observed in the simulations. As can be seen from Table I, the differences in the transport level reduce with increasing shear parameter $\hat{s}$. For moderate or high shear, $\hat{s} > 1$, the suppression is only about 10% or less, i.e., of the order of the statistical uncertainties $\Delta\Gamma_n/\Gamma_n$ observed in the simulations. Thus the effect of nonlinear electron Landau damping can be neglegted for collisionless drift-wave turbulence if and only if the magnetic shear is high enough, $\hat{s} > 1$, whereas for low shear, $\hat{s} < 1$, it can suppress the resulting turbulent transport significantly. As has been explained, this behavior is a consequence of the nonlinear drive mechanism. In the unsheared case, the subtle balance between the drift waves and the convective cells makes the system quite sensitive with respect to changes in the parallel electron dynamics, whereas for finite shear, n and ϕ are directly coupled to each other through a nonzero $k_{\|}$.

So our results show that in a tokamak edge ($r/a > 0.8$) where generally $\hat{s} > 1$, nonlinear electron Landau damping does not need to be considered in the construction of transcollisional Landau-fluid models for nonadiabatic passing electron dynamics. Thus we have removed one potential source of disagreement between fully kinetic models and their less costly substitutes, Landau-fluid models. Nevertheless, nonlinear fluid models of collisionless drift-wave turbulence will still have to be compared against fully kinetic calculations like the present one in order to test their applicability in the strongly turbulent regime.

[1] P. C. Liewer, Nucl. Fusion **25**, 543 (1985).
[2] Z. Chang and J. D. Callen, Phys. Fluids B **4**, 1167 (1992).
[3] B. D. Scott, in *Proceedings of the 20th European Conference on Controlled Fusion and Plasma Physics* (European Physical Society, Lisbon, 1993), p. IV-1411.
[4] G. W. Hammett and F. W. Perkins, Phys. Rev. Lett. **64**, 3019 (1990).
[5] R. E. Waltz, R. R. Dominguez, and G. W. Hammett, Phys. Fluids B **4**, 3138 (1992).
[6] W. W. Lee, J. A. Krommes, C. R. Oberman, and R. A. Smith, Phys. Fluids **27**, 2652 (1984).
[7] R. D. Hazeltine and J. D. Meiss, *Plasma Confinement* (Addison-Wesley, Redwood City, CA, 1992).
[8] K. V. Roberts and J. B. Taylor, Phys. Fluids **8**, 315 (1965).
[9] R. L. Dewar and A. H. Glasser, Phys. Fluids **26**, 3038 (1983).
[10] M. A. Beer, S. C. Cowley, and G. W. Hammett, Phys. Plasmas **2**, 2687 (1995).
[11] B. D. Scott, Plasma Phys. Controlled Fusion **39**, 471 (1997).
[12] B. D. Scott, Phys. Fluids B **4**, 2468 (1992).
[13] D. Biskamp and A. Zeiler, Phys. Rev. Lett. **74**, 706 (1995).
[14] C. Z. Cheng and H. Okuda, Phys. Rev. Lett. **41**, 1116 (1978).
[15] B. D. Scott, Phys. Rev. Lett. **65**, 3289 (1990).
[16] J. F. Drake, A. Zeiler, and D. Biskamp, Phys. Rev. Lett. **75**, 4222 (1995).
[17] C. Z. Cheng and H. Okuda, Nucl. Fusion **18**, 587 (1978).
[18] T. H. Dupree, Phys. Fluids **9**, 1773 (1966).